

Effects of mitochondrial dynamics genes, *fzo-1* and *drp-1*, on dopaminergic neurodegeneration induced by environmental exposure in *Caenorhabditis elegans*, as a model of Parkinson's disease

Samantha Hall

Honors Thesis submitted in partial fulfillment of the requirements for graduation with Distinction in Biology and Environmental Sciences in Trinity College of Duke University.

under the supervision of Dr. Joel N. Meyer,
Nicholas School of the Environment, Duke University
Durham, North Carolina

April, 2015

Abstract

Parkinson's disease (PD) is caused by degeneration of the dopaminergic neurons; environmental toxicants are hypothesized to play a role in PD etiology. Environmental toxicants can cause mitochondrial dysfunction through mitochondrial DNA (mtDNA) damage and production of reactive oxygen species. Serial ultraviolet C (UVC) radiation causes an accumulation of mtDNA damage and 6-hydroxydopamine (6-OHDA) causes loss of dopaminergic neurons.

Mitochondrial dynamics, or fusion and fission of the mitochondria, are important processes in mitigating mitochondrial dysfunction. The *fzo-1* and *drp-1* genes in *Caenorhabditis elegans* are orthologs for human Mfn1/2 and Drp1 and are involved in mitochondrial fusion and fission, respectively. I tested the hypothesis that deletion mutant strains for these two genes would show increased neurodegeneration after environmental damage, relative to the wild-type control strain, due to the lack of normal mitochondrial dynamics. Unexpectedly, both the *fzo-1* and *drp-1* were protected against 6-OHDA-induced neurodegeneration relative to wild-type. The *fzo-1* knockout underwent complete larval arrest after UVC exposure, suggesting that mitochondrial fusion is necessary for recovery after mtDNA damage. The *drp-1* mutant showed slightly more neurodegeneration than wild-type after UVC exposure at the 10 J/m² dose, but not the 7.5 J/m² dose. These results highlight the significance of mitochondrial dynamics and gene-environment interactions in dopaminergic neurodegeneration and PD etiology.

Introduction

Parkinson's disease (PD) is a neurodegenerative disease of great interest and impact; its most notable symptoms include tremors, rigidity, and impaired gait. This disease is currently estimated to affect over 4 million people over age 50 worldwide, with that number predicted to double by 2030 (Dorsey *et al.*, 2007). Aside from the personal devastation it causes to a patient's quality of life, the economic cost of PD in the United States is estimated to be about \$10.8 billion annually (O'Brien *et al.*, 2009). PD is characterized by the loss of dopaminergic neurons in a specific region in the brain called the substantia nigra. Genetics alone are hypothesized to account for only roughly 10% of PD cases (Cannon & Greenamyre, 2011), though genes associated with early-onset familial PD like *parkin*, *dj1*, and *pink1* have clarified some of the mystery of PD. The causes of the other 90% of PD cases are unknown, but it is likely that environmental exposures play a very significant role (Cannon & Greenamyre, 2011). One kind of environmental exposure hypothesized to cause PD is exposure to dopaminergic neurotoxins (Dauer & Przedborski, 2003). Environmental toxicants may be especially relevant for more susceptible genetic backgrounds; gene-environment interactions may be responsible for why the same exposure results in disease in only a subset of people (Meyer *et al.*, 2013). Neurodegeneration may be elicited by mitochondrial dysfunction, rendering mitochondria an important object of study in determining how neurodegeneration occurs. Additionally, mitochondria are susceptible to environmental toxicants (Meyer *et al.*, 2013), and this may be the key in discovering how environmental factors cause PD. The following thesis delves into the complex interplay between environmental exposures, dopaminergic neurodegeneration, and mitochondrial dynamics that are hypothesized to ultimately lead to Parkinson's disease.

Neurodegeneration in the Dopaminergic Neurons

Neurodegeneration generally refers to the loss of structure or function of neurons, which can cause devastating mental and physical effects (Cannon & Greenamyre, 2011). One classic example in the PD literature demonstrated how an environmental exposure could cause the death of dopaminergic neurons, resulting in PD symptoms. MPTP (1-methyl-4-phenyl-1,2,3,6-tetrahydropyridine) was unintentionally produced as a contaminant in synthetic heroin in 1982 (Langston *et al.*, 1983). Drug users accidentally exposed to MPTP subsequently displayed a behavioral phenotype similar to Parkinson's disease and improved after being treated with standard PD medication (Langston *et al.*, 1983).

Later research revealed that MPTP can cross the blood-brain barrier and be metabolized to MPP⁺ (1-methyl-4-phenylpyridinium) (Javitch *et al.*, 1985). This active metabolite MPP⁺ can then enter dopaminergic neurons through the dopamine transport symptom (Javitch *et al.*, 1985). Once MPP⁺ reaches the dopaminergic neurons, it concentrates in the mitochondria, inhibits complex I of the electron transport chain, and causes cell dysfunction and cell death (Nicklas *et al.*, 1985). MPTP thus caused symptoms of parkinsonism through its MPP⁺ metabolite by destroying dopaminergic neurons. MPTP has since proven useful in animal models of PD (Smeyne & Jackson-Lewis, 2005) and its role as a complex I inhibitor highlights the crucial role of mitochondria in dopaminergic neurodegeneration and in PD.

The Growing Influence of Environmental Toxicants

From heavy metals to radiation to lead, environmental exposures have garnered great interest for their role in the etiology of diseases, including PD. Determining the influence of environmental toxicants is being recognized as an important part of elucidating how diseases develop and the mechanisms through how they work (Rappaport *et al.*, 2014). Environmental

toxicants can cause disease through damaging DNA, including mitochondrial DNA (mtDNA) (DiMauro & Davidzon, 2005).

Some of the specific environmental factors that are thought to be tied to PD include pesticides like rotenone (Tanner *et al.*, 2011), paraquat (Dinis-Oliveira *et al.*, 2006), and β -HCH (Richardson *et al.*, 2009). Pesticides that cause mitochondrial dysfunction and increase oxidative stress have been positively associated with PD in epidemiological studies (Tanner *et al.*, 2011). However, we are still far from a complete understanding of the environmental factors that contribute to Parkinson's disease.

There is a real gap in research with regards to environmental toxicants and their effects on mitochondria, as evidenced by the small, albeit increasing amount of literature. The importance of mitochondria and their unique susceptibility to damage render them essential objects of study in the context of environmental toxicology (Meyer *et al.*, 2013). Given the associations between pesticides that affect mitochondria and the development of PD, mitochondria are a key area of PD research.

The Essentiality of Mitochondria in Neurons

Neurons are particularly vulnerable to mitochondrial damage because of their dependence on mitochondria to sustain high rates of metabolic activity (Exner *et al.*, 2012). The loss of neurons is incredibly detrimental because neurons are difficult, even impossible to replace (Nowakowski, 2006). Mitochondria are extremely important for normal cell functioning because they generate ATP through oxidative phosphorylation. Mitochondria in neurons contribute in many different processes: Ca^{2+} homeostasis, regulating neurotransmitter release, neurogenesis, and neuronal plasticity (Nunnari & Suomalainen, 2012). Mitochondria also provide

intermediates from the Krebs cycle that are used to synthesize GABA and glutamate neurotransmitters (Nunnari & Suomalainen, 2012).

Mitochondria can be damaged through numerous means, such as mtDNA damage or reactive oxygen species. The mitochondrial genome is quite small in comparison to the nuclear genome, but mtDNA is more susceptible to damage from reactive oxygen species (Yakes & Van Houten, 1997). Mitochondria also lack crucial repair mechanisms. Because mitochondria do not possess a nucleotide excision repair system, mtDNA is particularly vulnerable to bulky DNA lesions, relative to nuclear DNA (Bess *et al.*, 2012; LeDoux *et al.*, 1992). Since these bulky helix-distorting DNA adducts cannot be repaired by the mitochondria, the mtDNA is more prone to misrepair and to mutations (Sinha & Häder, 2002). These bulky DNA adducts can also inhibit replication of the mitochondrial genome by inhibiting DNA polymerase γ , the only mtDNA polymerase (Meyer *et al.*, 2013). Due to the prevalence of mitochondria, mutations in mtDNA can cause detriments in every body tissue, such as the brain, heart, or muscle (DiMauro & Schon, 2003). Mitochondrial dysfunction caused by reactive oxygen species can also lead to neurodegeneration (Nunnari & Suomalainen, 2012). A variety of homeostatic processes can protect against mitochondrial damage and repair mitochondria such as mitophagy and – the focus of this thesis – mitochondrial dynamics.

Mitochondrial Dynamics

Mitochondrial dynamics, or the fission and fusion of mitochondria, are vital in maintaining healthy populations of mitochondria. Fusion involves two mitochondria joining into one mitochondrion (see **Figure 1A**), possibly as a compensatory mechanism for mild mitochondria damage (e.g., the two mitochondria can be mildly damaged in different ways, so by

joining, there is less overall detriment in function). Fission involves a single, possibly damaged mitochondrion dividing into two mitochondria (see **Figure 1B**); this process is helpful in getting rid of damage through mitophagy, the mitochondrial-specific form of autophagy that digests impaired mitochondria. Maintaining a functioning network of mitochondria thus requires a balance between these two processes (Green & Van Houten, 2011).

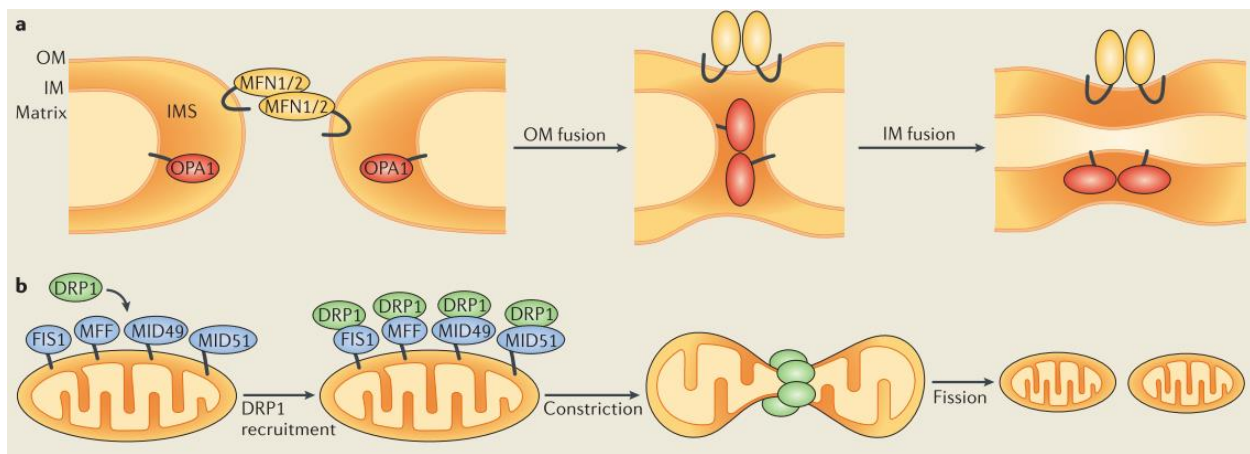


Figure 1: Mitochondrial fusion and fission | (A) Mitochondrial fusion involves two mitochondria coming together at the matrix. This is mediated by FZO-1 in *C. elegans* (human orthologs are Mfn1 and Mfn2). **(B)** Mitochondrial fission involves one mitochondria dividing into two. This is mediated by DRP-1. Adapted from Mishra and Chan (2014).

Mitochondrial dynamics are being studied as a therapeutic target for neurodegeneration – and specifically DRP-1 inhibition has shown promising results. Inhibition of DRP-1 has recently been found to attenuate neurotoxicity in mice (Rappold *et al.*, 2014). Inhibiting mitochondrial fission has also been found by other researchers to attenuate neurodegeneration (Cassidy-Stone *et al.*, 2008; Cui *et al.*, 2010; Lackner & Nunnari, 2010). The experiments of this thesis were done with knockouts of the *fzo-1* and *drp-1* genes, mitochondrial fusion and fission genes respectively, and were compared to a wild-type control strain (the BY250 strain).

FZO-1 is a protein that plays a role in the fusion of mitochondria. The Fzo homologs in humans are mitofusin (Mfn)1 and Mfn2; fibroblasts lacking in either Mfn1 or Mfn2 possess

fragmented mitochondria due to mitochondrial fusion deficiencies (Chen *et al.*, 2003). DRP-1 is a dynamin-related protein essential for most types of mitochondrial fission. Reductions in mitochondrial fission lead to elongated mitochondria.

Narrowing Down the Question of this Thesis

In this thesis I focus on two environmental exposures (UVC exposure and 6-OHDA exposure) and two different *Caenorhabditis elegans* strains with deletions in mitochondrial dynamics genes (*fzo-1* and *drp-1*). My control strain was the wild-type BY250 strain that contained no mitochondrial dynamics deficiencies. Ultraviolet C radiation or UVC has been found to cause an accumulation of mtDNA damage (Bess *et al.*, 2012). 6-hydroxydopamine or 6-OHDA is a synthetic neurotoxin predominantly used by researchers to selectively cause dopaminergic neurodegeneration. 6-OHDA is presumed to cause neurotoxicity through reactive oxygen species (Soto-Otero *et al.*, 2000) or as a complex I inhibitor (Glinka *et al.*, 1996). Although 6-OHDA is not a natural environmental exposure, it is used to model environmental insults and has been extensively used to study PD (Deumens *et al.*, 2002; Simola *et al.*, 2007). I conducted two different experiments on my *C. elegans* strains; first to observe neurodegeneration after exposure to 6-OHDA, and secondly to observe neurodegeneration after exposure to UVC.

I hypothesized that because the *fzo-1* and *drp-1* mutant strains were deficient in mitochondrial fusion and fission, there would be a difference in their capability (relative to wild-type) to recover from environmental damage induced by UVC and 6-OHDA. Thus, it was expected that the *fzo-1* and *drp-1* mutant strains would show more dopaminergic neurodegeneration, relative to the wild-type BY250 strain, after the environmental exposure.

More extensive dopaminergic neurodegeneration in the mutant strains could hold key insights in elucidating the etiology of PD, especially with regards to the role of mitochondria in PD as individuals with mitochondrial deficiencies could thus be more sensitive to the environmental exposures that lead to PD.

Methods

Model Organism: *Caenorhabditis elegans* is a useful model organism due to its short generation time, entirely sequenced genome, and complete cell lineage. *C. elegans* is particularly useful in studying neurodegeneration through the transgenic strain BY250, in which the dopaminergic neurons can be visualized with green fluorescent protein (GFP). *C. elegans* were maintained on food at 20 °C on K agar plates seeded with *E. coli* strain OP50. The BY250 strain, which expresses GFP only in the dopaminergic neurons, was generously provided by Michael Aschner. The *fzo-1* deletion strain was provided by Alexander van der Bliet and the *drp-1* deletion strain was provided by Ding Xue; these mutant strains were subsequently crossed with the wild-type BY250 strain.

Mutant Strain Generation: I crossed the *fzo-1* knockout strain and the *drp-1* knockout strain with the BY250 strain for use in neurodegeneration assays. I generated males from a mixed population of BY250 hermaphrodites by heat shock for 1 hour at 35 °C and raised them at the standard temperature of 20 °C. Hermaphrodites from the *fzo-1* knockout and *drp-1* knockout were subsequently placed singly on extra small K agar plates with BY250 males for mating in a

ratio of three BY250 males per one mutant hermaphrodite. I deemed the crossings successful if offspring from this mating (F1 generation) expressed green fluorescent protein (GFP) in their dopaminergic neurons under a fluorescent dissecting microscope. F1 offspring expressing GFP were individually placed on K agar plates and allowed to lay eggs. After laying eggs, the F1 generation was lysed and genotyped using PCR and gel electrophoresis to identify heterozygotes for the knockout condition (deletion in *fzo-1* or *drp-1*); only offspring from F1 heterozygotes were kept. Additional methods on the PCR and gel electrophoresis conditions used can be found in **Supplemental 1**. Individuals from the F2 generation that expressed GFP were individually placed on K agar plates and allowed to lay eggs. After laying eggs, the F2 generation was lysed and genotyped using PCR and gel electrophoresis to identify homozygotes for the knockout condition. In this manner, *fzo-1* and *drp-1* knockout strains with a Pdat-1::GFP background were generated.

UVC Exposure: The ultraviolet C (UVC) radiation dosing scheme used for worms in this experiment was developed by the Meyer Lab and was done as previously described (Bess *et al.*, 2012). Worms were first synchronized at the first larval stage (L1) and plated on to unseeded K agar plates without food or peptone (the exclusion of peptone was to prevent the growth of bacterial and fungal contaminants on the plates). The L1s were starved during the entire UVC exposure to inhibit worm growth. Strains were dosed three times with 7.5 or 10 J/m² of UVC radiation at 254 nm at 24-hour intervals (see **Figure 2**). This serial UVC exposure results in the accumulation of mitochondrial DNA damage (Bess *et al.*, 2012). The 24-hour intervals allowed for repair of nuclear DNA through nucleotide excision repair in between UVC doses. Mitochondria lack the nucleotide excision repair pathway to repair bulky helix-distorting lesions,

allowing for selective mtDNA damage (Bess *et al.*, 2012). After the third and final exposure, the worms were provided with food and allowed to develop.

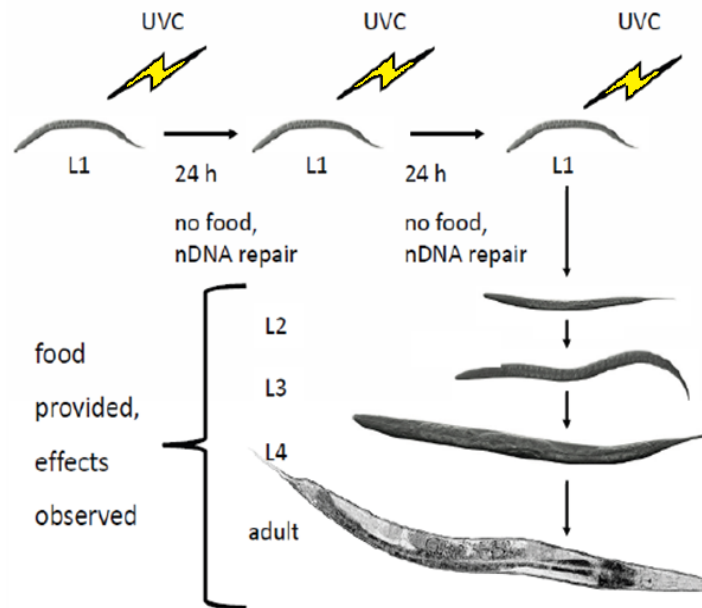


Figure 2: UVC dosing scheme for *C. elegans* developed by the Meyer Lab | Starved L1s (first larval stage) were exposed to ultraviolet C radiation three times at 24 hour intervals in order to accumulate mtDNA damage.

The sensitivity of the *fzo-1* strain to UVC was prohibitive to its use in neurodegeneration assays. Exposure of *fzo-1* to 7.5 and 10 J/m² resulted in complete larval arrest. Further exposures of *fzo-1* to other doses of UVC (1.25, 2.5, and 25 J/m²) and even different life stages (one dose at L1, one dose at L4, and others) were similarly unsuccessful; for unsuccessful and additional UVC experiments see **Supplemental 2**. This experiment tested BY250 (wild-type background), *fzo-1*, and *drp-1* under UVC exposure of 7.5 or 10 J/m² with unexposed controls. Neurodegeneration scoring took place after food was provided at the timepoints of 48 hours, 96 hours, and 9 days after providing food.

6-OHDA Exposure: The organic neurotoxin 6-hydroxydopamine (6-OHDA) was used to explore the sensitivity of dopaminergic (DA) neurons across the strains. 6-OHDA is a Parkinsonism-inducing neurotoxin that has been used to study toxin-mediated cell death and dopamine transport (Nass & Blakely, 2003). For the 6-OHDA exposure larval stage 4 (L4) worms were exposed to 50 mM or 100 mM 6-OHDA (Sigma-Aldrich) for 1 hour in liquid, and then placed on seeded K agar plates. The 6-OHDA was dissolved into an antioxidant, ascorbic acid (L-Ascorbic acid, Sigma-Aldrich); control treatments were only exposed to the ascorbic acid. Additional methods on the 6-OHDA exposure can be found in **Supplemental 3**. The BY250 and *drp-1* worms reached the L4 stage after 48 hours on food; the *fzo-1* worms, which develop slowly, reached the L4 stage after 72 hours on food. Synchronized *fzo-1* L1s were thus plated on food a day earlier than the other two strains to enable simultaneous blinded 6-OHDA dosing of all three strains at the L4 stage. Neurodegeneration scoring took place at 48 hours and 6 days after 6-OHDA exposure.

Slide Preparation: Worms for scoring were visualized under a Zeiss fluorescent compound microscope. Live worms were picked from plates on to slides on to a 2% agar pad and anesthetized with 10 μ L of 3 mM levamisole before placing a 1 mm thick coverslip and sealing the coverslip with nail polish (to prevent the coverslip from moving and to prevent the worms from drying out as quickly). While prepared slides were not in use, they were placed in a 4°C refrigerator. Confocal images were obtained on a Zeiss LSM 510 upright confocal microscope using stacks at 1 μ m intervals. Worms imaged for confocal microscopy were prepared with minor differences using 1.5 mm coverslips instead of 1 mm and sealed with tape rather than nail polish. In addition, 170 mM sodium azide was used to anesthetize worms for confocal

microscopy to achieve more complete paralysis than levamisole. To see the confocal images, as viewed with ImageJ software, see **Supplemental 4**.

Neurodegeneration Scoring: The neurodegeneration was quantified through blinded scoring (with both strain and dose unknown) of four dopaminergic neurons in the head, specifically the cephalic sensilla (CEP) dendrites on a scale from 0 to 2. Degeneration was measured through morphological changes – in this case, blebs and breaks (Nass *et al.*, 2002). Blebs are bulges in the cell membrane during processes such as apoptosis, and breaks are denoted by areas along the dendrite with no GFP expression (see **Figure 3**). The scoring scale used for neurodegeneration in *C. elegans* has been previously described (González-Hunt *et al.*, 2014). A score of 0 indicated no observable damage, 0.5 was blebbing but with 50% or more of the dendrite intact and no breaks, 1 was blebbing but with less than 50% of the dendrite intact and no breaks, 1.5 was breaks but with 50% or more of the dendrite still present, and 2 indicated the most damage with breaks and less than 50% of the dendrite present or complete degeneration. For neurodegeneration I did three repetitions of my experiments with 15 worms for each rep; thus 45 worms, or 180 neurons, were observed and blindly scored in total for each treatment (in both the UVC and the 6-OHDA exposures).

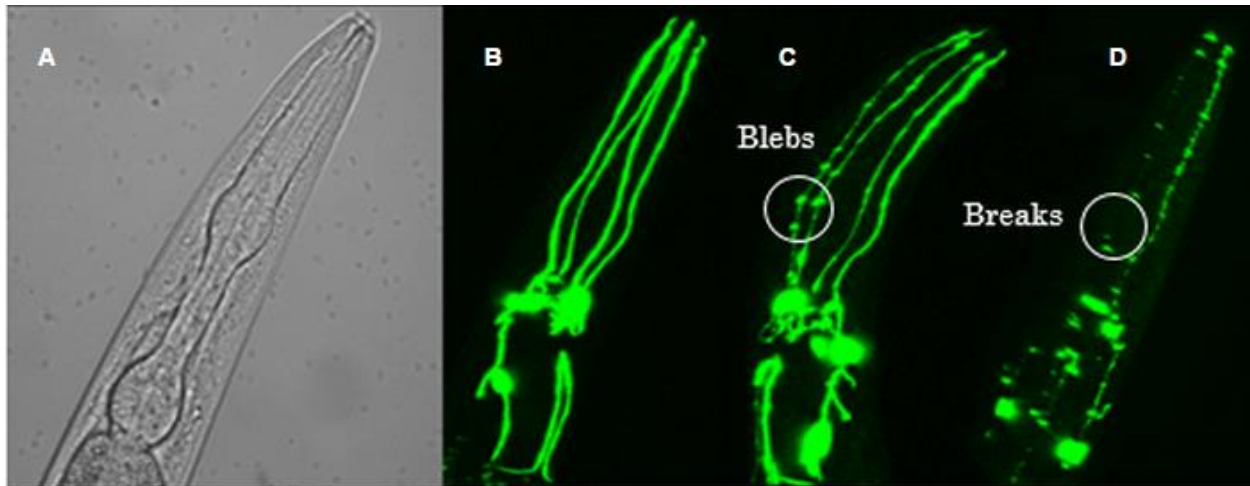


Figure 3: Neurodegeneration scoring scale | (A) The brightfield image on the left shows the head region of *C. elegans*. The head region of adult *C. elegans* is around 0.1-0.2 mm in length, with the total length of the worm being about 1 mm. (B) Fluorescent image showing the four cephalic dopaminergic neurons in an unexposed worm. (C and D) Two different worms exhibiting neurodegeneration in the form of blebs and breaks after exposure to 6-OHDA. The following describes what level of neurodegeneration warranted each score: 0, no noticeable damage; 0.5, blebs on $\leq 50\%$ of dendrite, no breaks; 1, blebs on $>50\%$ of dendrite, no breaks; 1.5, breaks, $\geq 50\%$ of dendrite still present; 2, breaks, $<50\%$ of dendrite present, includes completely absent dendrite.

Statistical Analysis: Dopaminergic neurodegeneration data were analyzed using the statistical software JMP Pro (Version 11.0.0, SAS Institute). The nonparametric Kruskal-Wallis test was used to test for differences between dosage levels of each exposure at each timepoint. Fisher's exact test was used to test the difference between the strains. A p -value of less than 0.05 was considered statistically significant. See **Supplemental 5** for tables listing all the statistics for all exposures and timepoints.

Results

Three different strains of *Caenorhabditis elegans*, BY250 (wild-type), *drp-1* (fission-deficient) and *fzo-1* (fusion-deficient), were tested to observe how much the dopaminergic neurons degenerate after exposure to an environmental insult, in the form of either 6-hydroxydopamine (6-OHDA) or ultraviolet C radiation (UVC) (see **Figure 4**). Neurodegeneration was observed on a compound fluorescent microscope and blindly scored on a scale of 0 to 2. A score of 0 indicated no observable damage, 0.5 was blebbing but with 50% or more of the dendrite intact and no breaks, 1 was blebbing but with less than 50% of the dendrite intact and no breaks, 1.5 was breaks but with 50% or more of the dendrite still present, and 2 indicated the most damage with breaks and less than 50% of the dendrite present or complete degeneration. Neurodegeneration scores are depicted through histograms to show the percentage of neurons with a certain score.

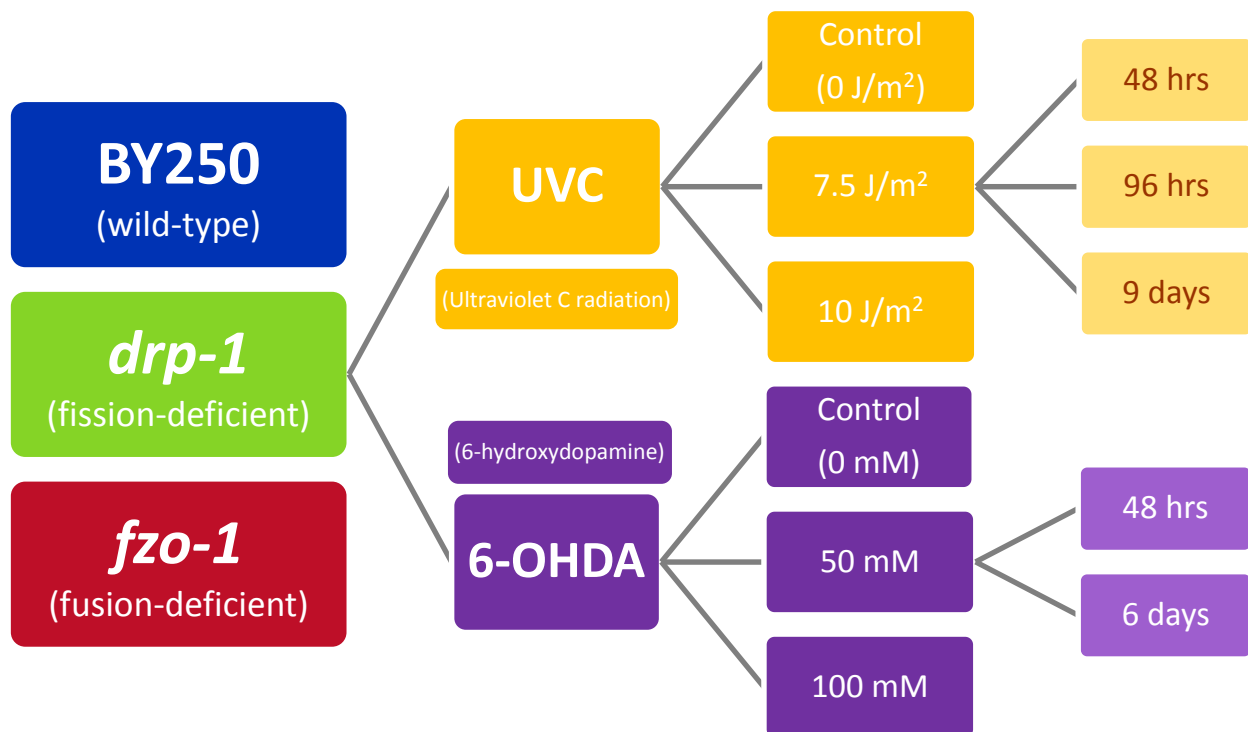


Figure 4: Experimental Design | This diagram shows the strains, environmental exposures, doses, and timepoints used in these experiments.

6-OHDA Exposure Results: Mutants for *fzo-1* and *drp-1* were protected from 6-OHDA-induced neurodegeneration, relative to wild-type

My first experiment consisted of exposing worms to the neurotoxin 6-hydroxydopamine (6-OHDA) and observing the subsequent neurodegeneration of four of the six dopaminergic neurons in the head. Larval stage 4 (L4) *Caenorhabditis elegans* were exposed to 6-OHDA and then scored at 48 hours and 6 days. Dosing was done three times for a total of three replicates. Within each strain, there is an effect of dose at both timepoints (p -value $< 0.0001^*$ for each strain, see **Figures 5 and 6**) – higher doses of 6-OHDA result in high levels of neurodegeneration (scores of 1.5 and 2) while the unexposed controls do not show neurodegeneration (scores of 0). Interestingly, the dose-response for 6-OHDA is bimodal, with 0 and 2 being the most frequent scores; it seems that 6-OHDA either resulted in complete neurodegeneration or in no effect. Between strains at the 48 hr timepoint, as seen in **Figure 7**, both mutant strains were unexpectedly protected against 6-OHDA-induced neurodegeneration; the *fzo-1* and *drp-1* exposed to 50 or 100 mM 6-OHDA have more neurons scored 0 and less neurons scored 2, relative to the wild-type BY250 (p -value $< 0.0001^*$ for 50 mM and 100 mM). However, at the 6 day timepoint the *drp-1* mutant shows levels of neurodegeneration similar to the wild-type BY250; the *fzo-1* still surprisingly shows less neurodegeneration even at this late timepoint (p -value $< 0.0001^*$ for 50 mM and 100 mM).

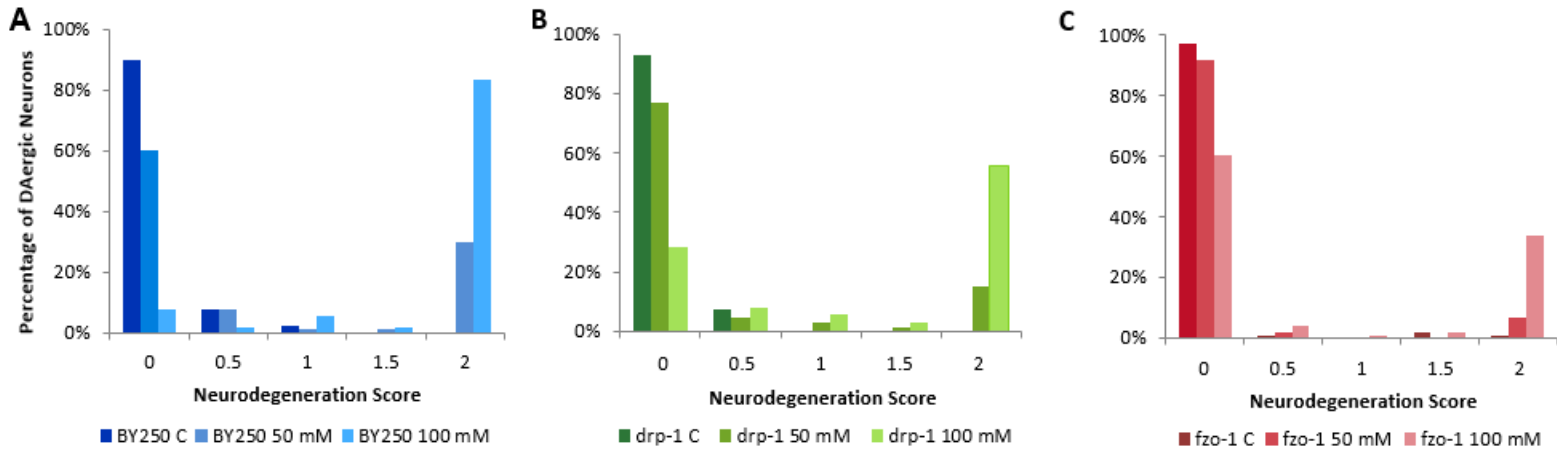


Figure 5: Neurodegeneration following 6-hydroxydopamine (6-OHDA) exposure 48 hours after dosing | Each treatment group had the four cephalic neurons of 45 worms scored, for $n = 180$ per treatment. Percentage is out of the 180 neurons per treatment with that respective score. **(A)** BY250 or wild-type strain dose response. **(B)** *drp-1* mutant strain dose response. **(C)** *fzo-1* mutant strain dose response. Every strain shows increased neurodegeneration at higher doses of 6-OHDA (p -value $< 0.0001^*$ for each strain). The BY250 (wild-type) shows the most extreme response, with almost 85% of the neurons completely degenerated at 100 mM of 6-OHDA. The *drp-1* and *fzo-1* were protected against 6-OHDA-induced neurodegeneration, showing less neurodegeneration at 50 mM and 100 mM of 6-OHDA (only 55% and 35% of neurons completely degenerating with 100 mM 6-OHDA; p -value $< 0.0001^*$ for 50 mM and 100 mM).

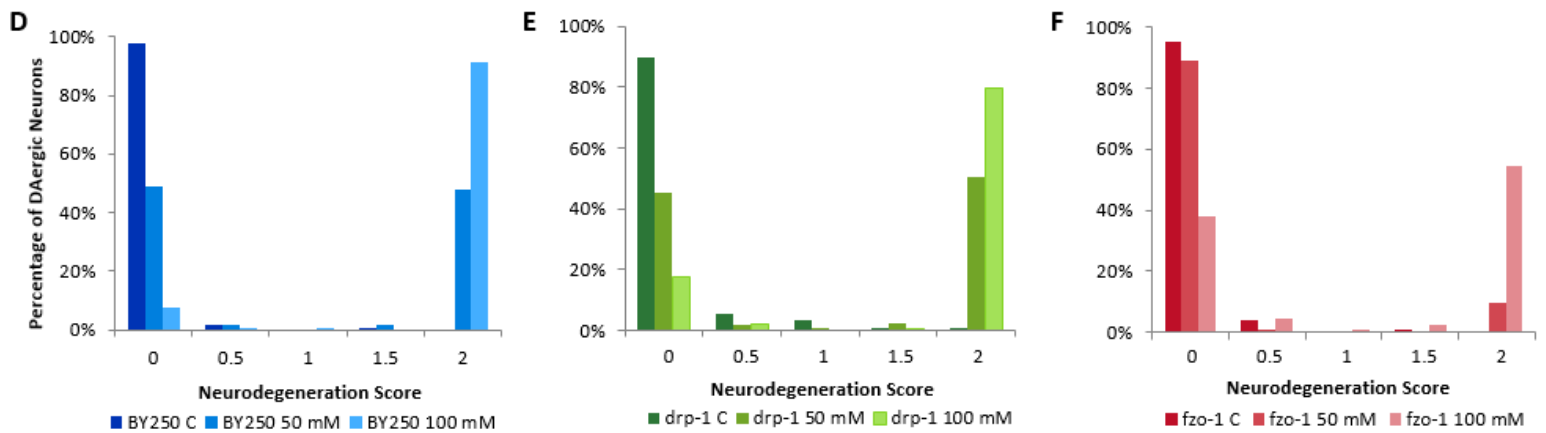


Figure 6: Neurodegeneration following 6-hydroxydopamine (6-OHDA) exposure 6 days (144 hours) after dosing | Each treatment group had the four cephalic neurons of 45 worms scored, for $n = 180$ per treatment. Percentage is out of the 180 neurons per treatment with that respective score. **(D)** BY250 or wild-type. **(E)** *drp-1* mutant strain response. **(F)** *fzo-1* mutant strain response. Every strain shows increased neurodegeneration at higher doses of 6-OHDA (p -value $< 0.0001^*$ for each strain). There was a difference between strains (p -value $< 0.0001^*$ for 50 mM and 100 mM) as the *fzo-1* was protected against the 6-OHDA; the *drp-1* showed levels of neurodegeneration similar to wild-type BY250.

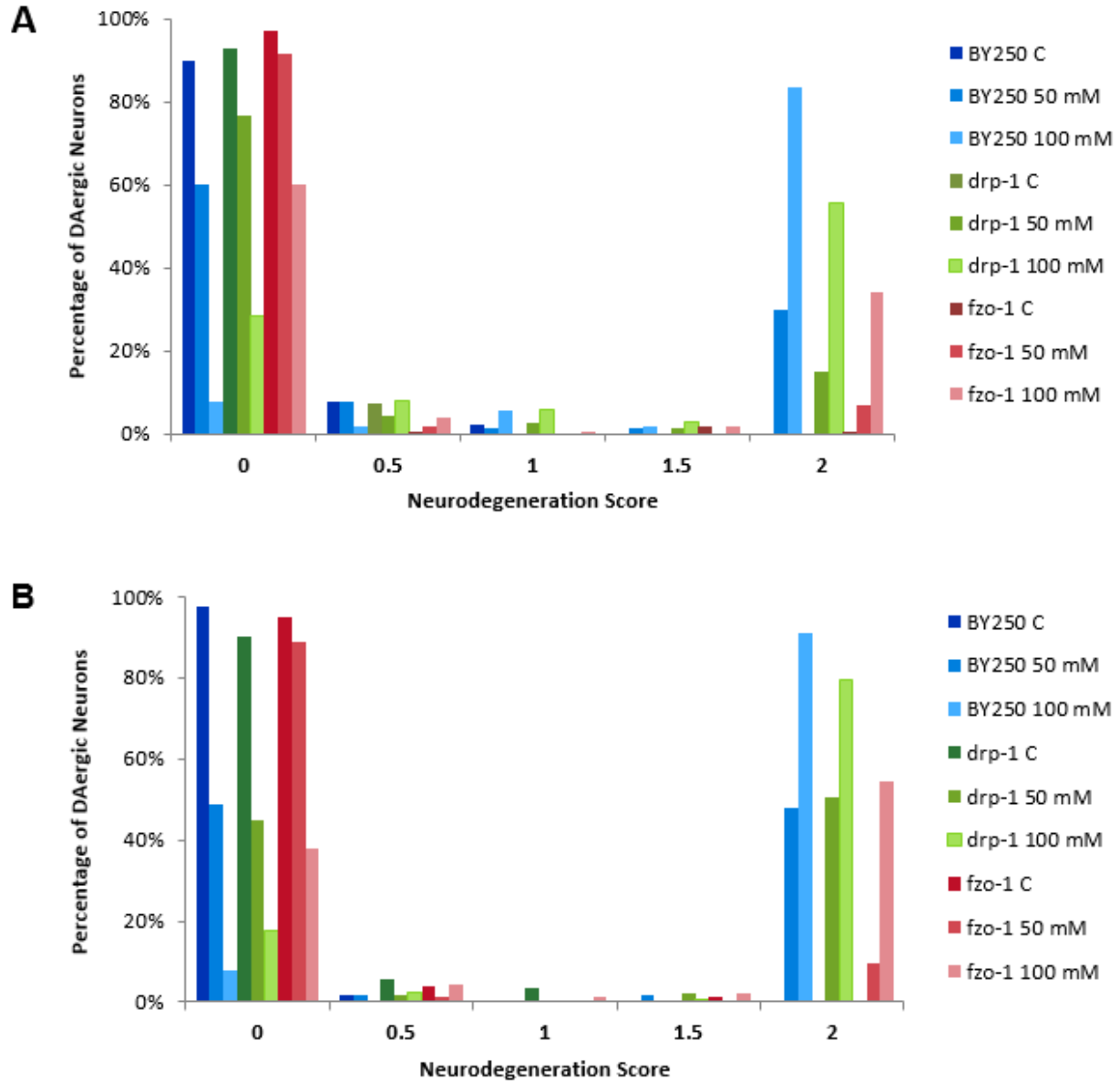
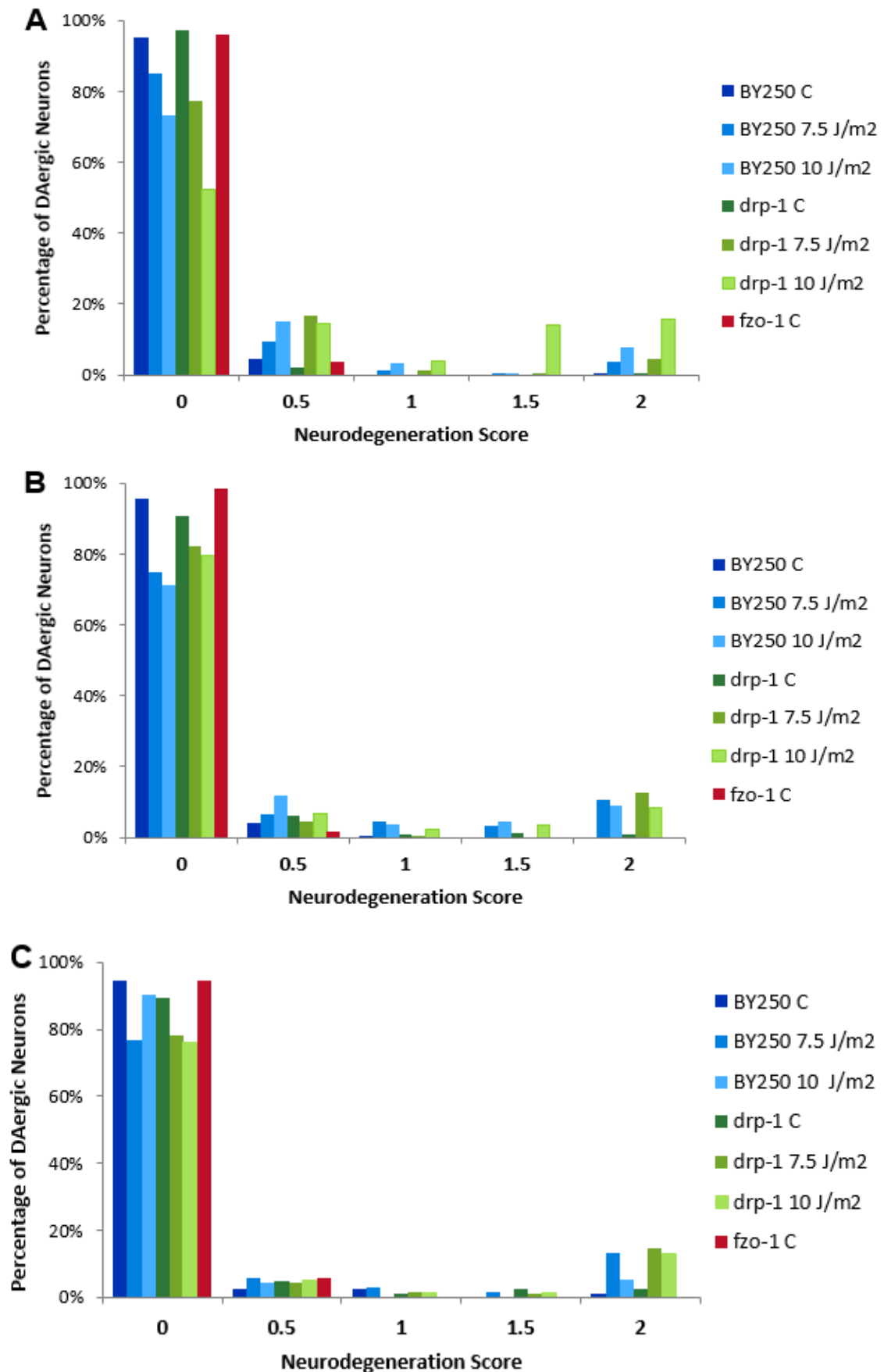


Figure 7: Neurodegeneration following 6-hydroxydopamine (6-OHDA) exposure | Another representation of the data presented in **Figures 5 and 6**, emphasizing the differences between the different strains and the different timepoints. **(A)** Scored 48 hours after 6-OHDA dosing. The *drp-1* and *fzo-1* were protected against the 6-OHDA, showing less neurodegeneration at 50 mM and 100 mM of 6-OHDA than the wild-type BY250. **(B)** Scored 144 hours (6 days) after 6-OHDA dosing. The *fzo-1* was protected against the 6-OHDA. The *drp-1* showed levels of neurodegeneration similar to wild-type BY250.

UVC Exposure Results: Mutant *fzo-1* are exceptionally sensitive while the mutant *drp-1* and BY250 are mildly affected

My second experiment consisted of exposing worms to ultraviolet C radiation (UVC) and observing the subsequent neurodegeneration of four of the six dopaminergic neurons in the head. Larval stage 1 (L1) *Caenorhabditis elegans* were exposed to UVC and then scored at 48 hours, 96 hours, and 9 days (see **Figure 8**). Dosing was done three times for a total of three replicates. The *fzo-1* underwent complete larval arrest after the UVC exposure and thus could not be scored. Within the *drp-1* and BY250 strains, there is an effect of dose at all three timepoints (p -value < 0.0001* for BY250; p -value < 0.0001* - 0.0047* for *drp-1*). UVC exposure caused less extensive neurodegeneration than the 6-OHDA exposure, as seen by the dose-response being shifted towards the 0 score. Between strains at the 48 hr and 9 day timepoints, the *drp-1* shows more neurodegeneration than the BY250 at the 10 J/m² dose (p -value < 0.0001* for 48 hours; p -value = 0.0222* at 9 days). At the 96 hr timepoint, there is an effect of strain at the 7.5 J/m² dose but not 10 J/m² dose (p -value = 0.0071* for 7.5 J/m²; p -value = 0.3515 for 10 J/m²).

Figure 8:
Neurodegeneration following ultraviolet C (UVC) exposure | Each treatment group had the four cephalic neurons of 43-60 worms scored, for $n = 168-240$ per treatment. Percentage represents the percentage of the neurons per treatment with that respective score. Dosing was done three times for a total of three replicates. Larval stage L1 *C. elegans* were exposed to UVC as described in the Methodology Section and then scored at three timepoints. BY250 (wild-type), *drp-1*, and *fzo-1* are different strains of *C. elegans*. The *fzo-1* underwent complete larval arrest following the UVC exposure and were unable to be scored. **(A)** Scored 48 hours after completion of UVC dosing. The *drp-1* showed sensitivity to UVC. **(B)** Scored 96 hours (2 days) after completion of UVC dosing. The *drp-1* showed levels of neurodegeneration similar to wild-type BY250. **(C)** Scored 216 hours (9 days) after completion of UVC dosing. The *drp-1* showed levels of neurodegeneration similar to wild-type BY250 at 7.5 J/m² and more neurodegeneration at 10 J/m².



Discussion

Discussion of the 6-OHDA Results

In these experiments, the *drp-1* and *fzo-1* deletion *Caenorhabditis elegans* mutants were unexpectedly protected from neurodegeneration induced by 6-hydroxydopamine (6-OHDA), at 48 hours after exposure. 6-OHDA likely causes neurodegeneration through the production of reactive oxygen species (ROS). In the *fzo-1* (fusion-deficient) and *drp-1* (fission-deficient) mutants, it is possible that the deficiencies in mitochondrial fusion and fission protect against the damaging effects of 6-OHDA by preventing the mitochondrial dysfunction that ROS normally causes. Given how important mitochondrial fission is for mitophagy, I hypothesized that *drp-1* would show more neurodegeneration after 6-OHDA exposure instead of less neurodegeneration. However, this surprising result supports a recent conclusion from Rappold *et al.* (2014) that inhibiting DRP-1 attenuates neurotoxicity in mice, by reducing cell death and even restoring dopamine release in a Parkinson's disease (PD) mouse model. Other studies in cells have also shown a neuroprotective role of DRP-1 inhibition. Inhibiting DRP-1 in HeLa cells partially protected the cells against cell death (Jagasia *et al.*, 2005) and inhibiting DRP-1 in *Drosophila* cells resulted in delayed mitochondrial fragmentation and cell death (Abdelwahid *et al.*, 2007).

As the results from 6-OHDA exposure at 6 days show, the *drp-1* and wild-type BY250 show similar levels of neurodegeneration from 6-OHDA exposure; thus, the *drp-1* got worse over time in regards to neurodegeneration. I hypothesize that while the *drp-1* is protected against neurodegeneration in early life relative to wild-type (e.g., at 48 hours), it eventually reaches equal or worse levels of neurodegeneration than the wild-type in later life (e.g., at 6 days). Mitochondrial fission is critical for mitophagy and maintaining the structural integrity of

mitochondria; I expect at some point that the detriment of inhibiting this important process will manifest, such as later in life as mitochondrial damage accumulates. As the scoring only went out to 6 days after exposure, a limitation of this experiment lies in the timepoints observed – neurodegeneration observed at 11 or 12 days may have shown that *drp-1* is worse than wild-type BY250.

The *fzo-1* deletion mutant, like the *drp-1*, was surprisingly also protected from 6-OHDA-induced neurodegeneration. However, this is in strong contrast with the ultraviolet C radiation (UVC) exposure results – these are discussed in more detail below. The *fzo-1* appears to be more protected than either *drp-1* or wild-type to 6-OHDA-induced neurodegeneration. Enhanced fission creates smaller mitochondria (which aids in the transportation of these mitochondria along the neuron) and aids in removing damaging mitochondria (Simcox *et al.*, 2013). Perhaps inhibiting mitochondrial fusion is protective after 6-OHDA exposure but not UVC exposure – UVC may cause more mitochondrial dysfunction and is broader in its toxicity than 6-OHDA, and fusion-deficient mutants just cannot recover from such high amounts of mtDNA damage.

Discussion of the UVC Results

The *drp-1* mutant showed neurodegeneration due to UVC exposure (but much less than in the 6-OHDA exposure), possibly because the lack of fission and the enhanced fusion compensates for the mitochondrial DNA damage. As neurodegeneration increases with aging, it is possible that the detrimental effects of UVC exposure on *drp-1* deletion mutants are not seen at early timepoints.

The extreme sensitivity of the *fzo-1* strain under UVC exposure was surprising. The *fzo-1* strain had a very strong response to UVC exposure, even under relatively low exposure, which

was not seen in either the BY250 or *drp-1* strains. The *fzo-1* underwent complete larval arrest as a response to UVC exposure and was thus mostly unusable for neurodegeneration scoring; limited scoring was done on the few worms that survived (albeit clearly not developing normally) after 24 hours on food, and these showed extensive neurodegeneration (i.e., scores of 1.5 and 2). This result suggests that mitochondrial fusion is critically necessary for recovery after UVC-induced mtDNA damage. However, it is always possible with mutant strains of *C. elegans* that there are other mutations involved. To rule out the possibility of the involvement of other mutations, the *fzo-1* strain could be further outcrossed with the wild-type to eliminate extraneous mutations or an RNAi (RNA interference) knockdown could be done to knockdown the *fzo-1* gene in the wild-type strain. If the extreme sensitivity to UVC exposure still held up, then that would provide stronger evidence for the essentiality of the *fzo-1* gene in recovery from mtDNA damage. With the current *fzo-1* deletion mutant, any dose and any dosing scheme results in larval arrest. The *fzo-1* was exposed to extensive UVC dosing at a wide range of doses (1.25, 2.5, 7.5, 10, and 25 J/m²) and at a wide range of developmental stages (three doses as starved L1s, one dose at L1, one dose at L4, multiple doses throughout L1 to L4). Regardless of dose or dosing scheme, the *fzo-1* mutant exhibited complete arrest. Exposure at later life stages (e.g., L4) seemed to delay the complete arrest by about 24 hours, but the animals still displayed a marked and abnormal decline in movement.

The UVC exposure results are difficult to interpret. I hypothesized that the mtDNA damage induced by UVC would cause noticeable levels of neurodegeneration. However, I did not expect the *fzo-1* mutant to be so incredibly sensitive to UVC exposure. Previous research showed that RNAi knockdown of the *fzo-1* gene eliminates the removal of UVC-induced mtDNA damage (Bess *et al.*, 2012). This fits well with the results of complete larval arrest of

the *fzo-1* deletion mutant after UVC – because it cannot remove the mtDNA damage, it fails to develop normally. However, an RNAi knockdown of the *drp-1* gene also eliminated the removal of UVC-induced mtDNA damage, leading to the question of why *drp-1* shows similar levels of neurodegeneration with the wild-type BY250. It is possible that removal of the mtDNA damage through mitophagy is not as necessary in the *drp-1* mutants because the enhanced mitochondrial fusion allows for functional complementation. With regards to the *fzo-1* mutant strain, mitofusins have other roles besides promoting mitochondrial fusion (Chen *et al.*, 2003); it is possible that an additional role of FZO-1, which may not even be known yet, is responsible for the *fzo-1* mutant's hypersensitivity to UVC exposure. The inhibition of fusion may lead to increased mitophagy (perhaps triggering more cell death) or to the compensatory upregulation of other protective mechanisms.

Future Directions

Continue work with DRP-1 and FZO-1: The results of this thesis confirm previous studies in the importance of DRP-1 in protection against dopaminergic neurodegeneration induced by environmental exposures. DRP-1 needs to be further studied both for its potential role in the causation of PD and for its possible therapeutic role in PD. As far as FZO-1, the unique sensitivity of the *fzo-1* mutant strain to UVC, coupled with its resistance to 6-OHDA-induced neurodegeneration, introduces many important questions. Why is one environmental exposure so incredibly detrimental while the other is not? Why is fusion so essential to mtDNA damage recovery but fission is not? While these questions may not all pertain to neurodegeneration or to PD etiology, the role of mitochondrial fusion needs to be further explored.

Morphology of Mitochondria in the Neurons: While I have confocal images of the dopaminergic neurons, I do not have images that show the mitochondrial morphology in those neurons. Showing the difference in mitochondrial morphology due to the inhibition of normal mitochondrial dynamics would enhance my results. A crucial future direction will be to utilize mitochondrion-selective fluorescent proteins or dyes to look at mitochondria, specifically the mitochondria in the four dopaminergic neurons that I scored. For the *fzo-1* deletion mutant, I would expect to see small, fragmented mitochondria due to the lack of mitochondrial fusion. For the *drp-1* deletion mutant, I would expect to see hyperfused mitochondria due to the lack of mitochondrial fission.

Additional Environmental Exposures: While 6-OHDA and UVC are good models for environmental toxicants, there are many other exposures that need to be tested – namely the typical pesticides used for PD studies, rotenone and paraquat. These two pesticides have been epidemiologically linked to PD (Tanner *et al.*, 2011). It will also be crucial to explore other relevant environmental exposures that are not as well-studied, such as the pesticides maneb or β -hexachlorocyclohexane. Finally, mixtures of environmental toxicants should be explored; people are not exposed to single chemical exposures but to a huge variety of different mixtures. While challenging, studying the effects of mixtures on neurodegeneration will be crucial.

Antioxidants: As 6-OHDA is hypothesized to cause neurodegeneration through the production of reactive oxygen species, adding antioxidants would enhance these experiments. If the addition of antioxidants has a protective effect, then it would suggest that ROS are important in the degeneration of the dopaminergic neurons. It is possible that there is ROS-related signaling

altering gene expression – perhaps a combination of the deficits in mitochondrial dynamics and ROS lead to the neuroprotective phenotype.

Behavioral Endpoints: Mouse and fish models of PD have previously been utilized to look at changes in behavior. Mice can show loss of motor function and cognitive impairment (Li *et al.*, 2013) while reduced locomotor activity (Flinn *et al.*, 2008) and deficits in spatial memory (Bortolotto *et al.*, 2014) have been seen in zebrafish models of PD. Medaka fish show PD-like symptoms through reduced spontaneous swimming movements (Matsui *et al.*, 2012). Ideally, studying the behavior of *C. elegans* will make *C. elegans* a more robust model of PD. Dopamine plays a role in locomotion and egg-laying in *C. elegans*; basal slowing response and area-restricted search are two behaviors that *C. elegans* exhibit to maximize their feeding (Schmidt *et al.*, 2007). Although *C. elegans* are much simpler in their behavior than fish or mice, studying and quantifying decreased feeding, increased locomotion, or dysfunctional egg-laying can provide insights into how dopaminergic neurodegeneration visible on a microscope translates into behavioral deficits.

Later Timepoints: As PD is a disease that occurs in later life, experiments with *C. elegans* should highlight the later timepoints. The farthest timepoint studied in this thesis is 9 days after exposure. The typical lifespan of wild-type *C. elegans* in the laboratory is two to three weeks. It is expected that neurodegeneration will increase as the worms age; however, very sudden or increased rates of neurodegeneration would be notable. Timepoints in the future should include 11-12 days after dosing if possible. Later life should also be a much more relevant timepoint for observation because PD is a neurodegenerative disease primarily affecting the elderly.

Additional Dosing Schemes: Larval stage 1 (L1) worms were used for the UVC exposure, but the slightly older larval stage 4 (L4) worms were used for the 6-OHDA experiment. L1s were not used for the 6-OHDA exposure because the *fzo-1* is slow-growing and blinded scoring could not be done (due to the notably smaller size of the *fzo-1* relative to the other strains). However, it is possible that exposing worms at different times will produce different results. Thus, L1s should be exposed to 6-OHDA and L4s should be exposed to UVC. Note that I did dose *fzo-1* at the L4 stage with UVC (see **Supplemental 2**) and the *fzo-1* still underwent complete larval arrest. It will also be interesting to try dosing schemes where there is an “early hit” at the L1 stage and a second “later hit” during adulthood. The early hit may either sensitize or protect the worm against damage from further hits. Transgenerational dosing schemes can also be explored, whereby parental exposure to a toxicant results in effects that affect future generations.

This thesis underscores the importance of mitochondrial dynamics and gene-environment interactions in the neurodegenerative response to detrimental environmental exposures. The results of this thesis show that fission-deficient *drp-1* and fusion-deficient *fzo-1* mutant strains of *Caenorhabditis elegans* primarily showed less neurodegeneration than the wild-type after environmental insult. Through more research, especially with DRP-1 and mitochondrial fission, the role of mitochondrial dynamics and environmental factors in dopaminergic neurodegeneration and Parkinson’s disease etiology can be elucidated.

Acknowledgements

I would like to thank my PI and research supervisor, Dr. Joel Meyer, for being an outstanding mentor during my four years at Duke. Being a part of his lab and classes has allowed me to find my passion in environmental health and toxicology, and I am grateful for all the advice and opportunities he has given me. Thank you, Joel, for all the work you have done for me, from recommendation letters to one-on-one meetings to being the best PI I could have asked for.

I would also like to especially thank Claudia González-Hunt for guiding me throughout my independent research project. She was a fantastic and inspirational teacher who was always there for me whenever I had questions, and I am so fortunate that she took the time to show me everything I needed to know. Thank you, Claudia, for sharing your enthusiasm about science and your infinite wisdom.

I would also like to thank all the current and former members of the Meyer Lab who helped shape my research experience over the past two and a half years. Thank you all for welcoming me into the lab as an undergrad and helping me progress past plate-pouring and washing tubes.

I appreciate Dr. Alexander Motten, Dr. Julie Reynolds, Dr. Jason Dowd, and all of the students of Biology 495 for their invaluable feedback on drafts. I also thank Dr. Kathleen Smith for taking the time to serve as my Faculty Reader and to read over my drafts.

Thanks to Michael Aschner, Alexander van der Blik, and Ding Xue for generously providing *Caenorhabditis elegans* strains used in this work. I would like to thank Pfizer and the SOT Endowment Fund for providing me with travel support to present this research at the Society of Toxicology 2015 Annual Meeting in San Diego, CA. The work of this senior thesis was funded by the National Institute of Environmental Health Sciences, NIEHS (1R01-ES017540-01A2).

References

- Abdelwahid, E., Yokokura, T., Krieser, R. J., Balasundaram, S., Fowle, W. H., & White, K. (2007). Mitochondrial Disruption in Drosophila Apoptosis. *Dev Cell*, *12*(5), 793-806.
- Bess, A. S., Crocker, T. L., Ryde, I. T., & Meyer, J. N. (2012). Mitochondrial dynamics and autophagy aid in removal of persistent mitochondrial DNA damage in *Caenorhabditis elegans*. *Nucleic Acids Res*, *40*(16), 7916-7931.
- Bortolotto, J. W., Cognato, G. P., Christoff, R. R., Roesler, L. N., Leite, C. E., Kist, L. W., Bogo, M. R., Vianna, M. R., & Bonan, C. D. (2014). Long-term exposure to paraquat alters behavioral parameters and dopamine levels in adult zebrafish (*Danio rerio*). *Zebrafish*, *11*(2), 142-153.
- Cannon, J. R., & Greenamyre, J. T. (2011). The Role of Environmental Exposures in Neurodegeneration and Neurodegenerative Diseases. *Toxicol Sci*, *124*(2), 225-250.
- Cassidy-Stone, A., Chipuk, J. E., Ingeman, E., Song, C., Yoo, C., Kuwana, T., Kurth, M. J., Shaw, J. T., Hinshaw, J. E., Green, D. R., & Nunnari, J. (2008). Chemical inhibition of the mitochondrial division dynamin reveals its role in Bax/Bak-dependent mitochondrial outer membrane permeabilization. *Dev Cell*, *14*(2), 193-204.
- Chen, H., Detmer, S. A., Ewald, A. J., Griffin, E. E., Fraser, S. E., & Chan, D. C. (2003). Mitofusins Mfn1 and Mfn2 coordinately regulate mitochondrial fusion and are essential for embryonic development. *J Cell Biol*, *160*(2), 189-200.
- Cui, M., Tang, X., Christian, W. V., Yoon, Y., & Tieu, K. (2010). Perturbations in Mitochondrial Dynamics Induced by Human Mutant PINK1 Can Be Rescued by the Mitochondrial Division Inhibitor mdm1. *J Biol Chem*, *285*(15), 11740-11752.
- Dauer, W., & Przedborski, S. (2003). Parkinson's Disease: Mechanisms and Models. *Neuron*, *39*(6), 889-909.
- Deumens, R., Blokland, A., & Prickaerts, J. (2002). Modeling Parkinson's Disease in Rats: An Evaluation of 6-OHDA Lesions of the Nigrostriatal Pathway. *Exp Neurol*, *175*(2), 303-317.
- DiMauro, S., & Davidzon, G. (2005). Mitochondrial DNA and disease. *Ann Med*, *37*(3), 222-232.
- DiMauro, S., & Schon, E. A. (2003). Mitochondrial Respiratory-Chain Diseases. *N Engl J Med*, *348*(26), 2656-2668.
- Dinis-Oliveira, R. J., Remião, F., Carmo, H., Duarte, J. A., Navarro, A. S., Bastos, M. L., & Carvalho, F. (2006). Paraquat exposure as an etiological factor of Parkinson's disease. *Neurotoxicology*, *27*(6), 1110-1122.

- Dorsey, E. R., Constantinescu, R., Thompson, J. P., Biglan, K. M., Holloway, R. G., Kieburtz, K., Marshall, F. J., Ravina, B. M., Schifitto, G., Siderowf, A., & Tanner, C. M. (2007). Projected number of people with Parkinson disease in the most populous nations, 2005 through 2030. *Neurology*, *68*(5), 384-386.
- Exner, N., Lutz, A. K., Haass, C., & Winklhofer, K. F. (2012). *Mitochondrial Dysfunction in Parkinson's Disease: Molecular Mechanisms and Pathophysiological Consequences* (Vol. 31).
- Flinn, L., Bretau, S., Lo, C., Ingham, P. W., & Bandmann, O. (2008). Zebrafish as a new animal model for movement disorders. *J Neurochem*, *106*(5), 1991-1997.
- Glinka, Y., Tipton, K. F., & Youdim, M. B. H. (1996). Nature of Inhibition of Mitochondrial Respiratory Complex I by 6-Hydroxydopamine. *J Neurochem*, *66*(5), 2004-2010.
- González-Hunt, C. P., Leung, M. C. K., Bodhicharla, R. K., McKeever, M. G., Arrant, A. E., Margillo, K. M., Ryde, I. T., Cyr, D. D., Kosmaczewski, S. G., Hammarlund, M., & Meyer, J. N. (2014). Exposure to Mitochondrial Genotoxins and Dopaminergic Neurodegeneration in *Caenorhabditis elegans*. *PLOS ONE*, *9*(12), e114459.
- Green, D. R., & Van Houten, B. (2011). Mitochondrial Quality Control. *Cell*, *147*(4), 950-950.e951.
- Jagasia, R., Grote, P., Westermann, B., & Conradt, B. (2005). DRP-1-mediated mitochondrial fragmentation during EGL-1-induced cell death in *C. elegans*. *Nature*, *433*(7027), 754-760.
- Javitch, J. A., D'Amato, R. J., Strittmatter, S. M., & Snyder, S. H. (1985). Parkinsonism-inducing neurotoxin, N-methyl-4-phenyl-1,2,3,6-tetrahydropyridine: uptake of the metabolite N-methyl-4-phenylpyridine by dopamine neurons explains selective toxicity. *PNAS*, *82*(7), 2173-2177.
- Lackner, L. L., & Nunnari, J. (2010). Small molecule inhibitors of mitochondrial division: tools that translate basic biological research into medicine. *Chem Biol*, *17*(6), 578-583.
- Langston, J. W., Ballard, P., Tetrud, J. W., & Irwin, I. (1983). Chronic Parkinsonism in Humans due to a Product of Meperidine-Analog Synthesis. *Science*, *219*(4587), 979-980.
- LeDoux, S. P., Wilson, G. L., Beecham, E. J., Stevnsner, T., Wassermann, K., & Bohr, V. A. (1992). Repair of mitochondrial DNA after various types of DNA damage in Chinese hamster ovary cells. *Carcinogenesis*, *13*(11), 1967-1973.
- Li, X., Redus, L., Chen, C., Martinez, P. A., Strong, R., Li, S., & O'Connor, J. C. (2013). Cognitive Dysfunction Precedes the Onset of Motor Symptoms in the MitoPark Mouse Model of Parkinson's Disease. *PLOS ONE*, *8*(8), e71341.
- Matsui, H., Gavinio, R., & Takahashi, R. (2012). Medaka Fish Parkinson's Disease Model. *Exp Neurobiol*, *21*(3), 94-100.

- Meyer, J. N., Leung, M. C. K., Rooney, J. P., Sandoel, A., Hengartner, M. O., Kisby, G. E., & Bess, A. S. (2013). Mitochondria as a Target of Environmental Toxicants. *Toxicol Sci*
- Mishra, P., & Chan, D. C. (2014). Mitochondrial dynamics and inheritance during cell division, development and disease. *Nat Rev Mol Cell Biol*, 15(10), 634-646.
- Nass, R., & Blakely, R. D. (2003). The *Caenorhabditis elegans* dopaminergic system: Opportunities for Insights into Dopamine Transport and Neurodegeneration. *Annu Rev Pharmacol Toxicol*, 43(1), 521-544.
- Nass, R., Hall, D. H., Miller, D. M., & Blakely, R. D. (2002). Neurotoxin-induced degeneration of dopamine neurons in *Caenorhabditis elegans*. *PNAS*, 99(5), 3264-3269.
- Nicklas, W. J., Vyas, I., & Heikkila, R. E. (1985). Inhibition of NADH-linked oxidation in brain mitochondria by 1-methyl-4-phenyl-pyridine, a metabolite of the neurotoxin, 1-methyl-4-phenyl-1,2,5,6-tetrahydropyridine. *Life Sci*, 36(26), 2503-2508.
- Nowakowski, R. S. (2006). Stable neuron numbers from cradle to grave. *PNAS*, 103(33), 12219-12220.
- Nunnari, J., & Suomalainen, A. (2012). Mitochondria: In Sickness and in Health. *Cell*, 148(6), 1145-1159.
- O'Brien, J. A., Ward, A., Michels, S. L., Tzivelekis, S., & Brandt, N. J. (2009). Economic burden associated with Parkinson disease in the United States. *Drug Benefit Trends*, 21(6), 179-190.
- Rappaport, S. M., Barupal, D. K., Wishart, D., Vineis, P., & Scalbert, A. (2014). The blood exposome and its role in discovering causes of disease. *Environ Health Perspect*, 122(8), 769-774.
- Rappold, P. M., Cui, M., Grima, J. C., Fan, R. Z., de Mesy-Bentley, K. L., Chen, L., Zhuang, X., Bowers, W. J., & Tieu, K. (2014). Drp1 inhibition attenuates neurotoxicity and dopamine release deficits in vivo. *Nat Commun*, 5
- Richardson, J. R., Shalat, S. L., Buckley, B., & et al. (2009). Elevated serum pesticide levels and risk of parkinson disease. *Arch Neurol*, 66(7), 870-875.
- Schmidt, E., Seifert, M., & Baumeister, R. (2007). *Caenorhabditis elegans* as a model system for Parkinson's Disease. *Neurodegener Dis*, 4(2-3), 199-217.
- Simcox, E. M., Reeve, A., & Turnbull, D. (2013). Monitoring mitochondrial dynamics and complex I dysfunction in neurons: implications for Parkinson's disease. *Biochem Soc Trans*, 41(6), 1618-1624.
- Simola, N., Morelli, M., & Carta, A. R. (2007). The 6-hydroxydopamine model of Parkinson's disease. *Neurotox Res*, 11(3-4), 151-167.

- Sinha, R. P., & Häder, D. P. (2002). UV-induced DNA damage and repair: a review. *Photochem Photobiol Sci*, 1(4), 225-236.
- Smeyne, R. J., & Jackson-Lewis, V. (2005). The MPTP model of Parkinson's disease. *Mol Brain Res*, 134(1), 57-66.
- Soto-Otero, R., Méndez-Álvarez, E., Hermida-Ameijeiras, Á., Muñoz-Patiño, A. M., & Labandeira-Garcia, J. L. (2000). Autoxidation and Neurotoxicity of 6-Hydroxydopamine in the Presence of Some Antioxidants. *J Neurochem*, 74(4), 1605-1612.
- Tanner, C. M., Kamel, F., Ross, G. W., Hoppin, J. A., Goldman, S. M., Korell, M., Marras, C., Bhudhikanok, G. S., Kasten, M., Chade, A. R., Comyns, K., Richards, M. B., Meng, C., Priestley, B., Fernandez, H. H., Cambi, F., Umbach, D. M., Blair, A., Sandler, D. P., & Langston, J. W. (2011). Rotenone, paraquat, and Parkinson's disease. *Environ Health Perspect*, 119(6), 866-872.
- Yakes, F. M., & Van Houten, B. (1997). Mitochondrial DNA damage is more extensive and persists longer than nuclear DNA damage in human cells following oxidative stress. *PNAS*, 94(2), 514-519.

Supplemental Information

Supplemental 1: PCR and Gel Electrophoresis for Crossing

Lysis: Worms that needed to be genotyped were individually picked from plates into 10 μL of lysis buffer. The tubes were then placed in the $-80\text{ }^{\circ}\text{C}$ for 10 minutes before being put into the thermocycler. As a note, I would make the lysis buffer for 10 worms in one batch in 10.2x quantity (thus, adding $8.2\text{ }\mu\text{L} \times 10.2$ of Sigma H₂O) and would pipette 10 μL of that batch into a small PCR tube (as opposed to trying to pipette individual amounts of 0.5 μL into all of my small tubes).

Lysis Buffer per worm

10x PCR buffer	1 μL
Qiagen proteinase K	0.5 μL
50 mM MgCl ₂	0.3 μL
Sigma H ₂ O	8.2 μL

Lysis 65 $^{\circ}\text{C}$ PCR Cycle

65.0	1 hour
95.0	15 min
8.0	Pause

Genotyping PCR: The Taq used for PCR was “Taq DNA Polymerase Recombinant 500 U (5U/ μL)” by Invitrogen. I used 49 μL of the Genotyping PCR master mix and 1 μL of the DNA lysate. I would always run the genotyping PCR immediately or within a few hours after my lysis. If you have to store the lysate before you run the genotyping PCR, I would suggest freezing it in the $-80\text{ }^{\circ}\text{C}$. Genotyping was most successful at 39 cycles (though 35-41 cycles were not that different). Possible modifications for troubleshooting include adding more lysate to the PCR (1 μL or 2 μL gave the best results); changing the number of cycles; and changing the concentration of MgCl₂ (50 mM was the best in my genotyping).

Genotyping PCR per worm

10x PCR buffer	5 μ L
dNTP	5 μ L
50 mMol MgCl ₂	3 μ L
F primer	1.5 μ L
R primer	1.0 μ L
Taq polymerase	1.0 μ L
Sigma H ₂ O	33.5 μ L
+DNA lysate	1 μ L

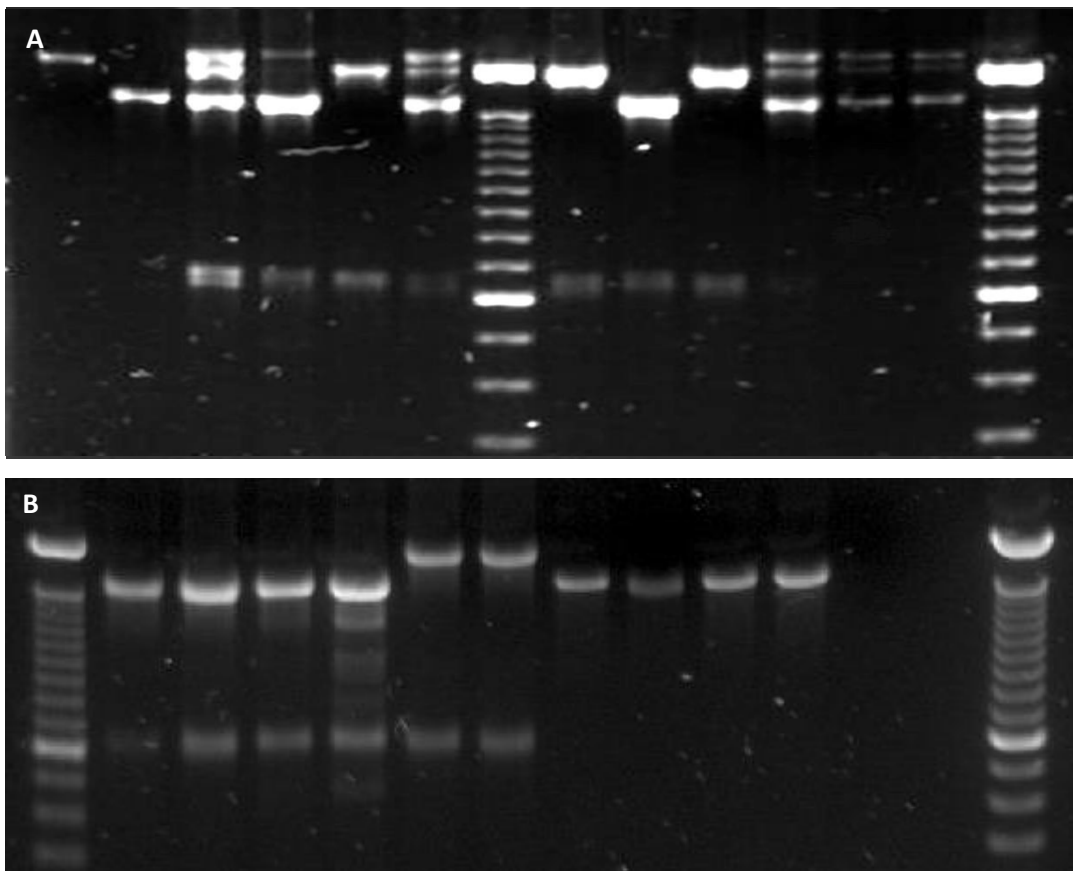
Genotyping PCR conditions

94.0	3 min
94.0	15 s
56.0	30 s
72.0	1 min 30 s (cycle back to Step 2 for however many cycles)
72.0	5 min
8.0	Pause

Primers: The working stock used for all primers was 10 μ M (diluted with Sigma H₂O from the 200 μ M stock). I would use 1.0 μ L instead of 1.5 μ L of each primer per worm when I would see strong primer dimers on my gels. The BC10210 *fzo-1* strain (tm1133) provided by Alexander van der Blik and the *drp-1* strain (tm1108) provided by Ding Xue were the strains I worked with; BY250 (provided by Michael Aschner) was used as my control. For the *fzo-1* I primarily used the external primers. I occasionally used the internal primers when I was troubleshooting my genotyping to be sure that I was amplifying that specific segment in the *fzo-1* gene. I had to order my own *drp-1* primers; the *drp-1* primers were developed by using WormBase (search for the variation “tm1108” and look for the Left and Right Oligo under tm1108_external; or check this link at wormbase.org/species/c_elegans/variation/WBVar00250125#02-45-3).

Before opening the *drp-1* primer stocks (the lyophilized powder), they were vortexed and then spun down. Then 0.1x TE was added to the primers to resuspend them. The primer stocks were repeatedly vortexed, then left overnight at 4 °C to hydrate. They were then heavily vortexed and spun down again. Working stocks were made and stored at 4 °C, and the primer stocks were stored at -20 °C

Gel Electrophoresis: Gels were made with 50 mL of 1% agarose (dissolved in TBE) and 5 μ L of Sybr-Safe. I liked using the well combs with smaller lanes (about 5 mm) because the bands were much clearer than bands with the larger lanes. TBE was the buffer (SB and TBA buffer worked as well, and there was very little difference). TrackIt Buffer (1 μ L) was used to load each sample (4 μ L) into gels. The ladder was 7 μ L of TrackIt 100 bp ladder. The gel was run at 150 V for approximately 30-40 minutes and then imaged with AlphaImager software. If there was not a clear separation between the bands yet, I would run the gel longer (for 1 hour of total running time). **Supplemental 1A and 1B** show representative gel images.



Supplemental 1: Gels of the F2 and F3 generations | (A) This gel shows the genotyping of the F2 generation. There are heterozygotes (lanes 3, 4, 6, and 11-13), wild-type homozygotes (lanes 1, 8, and 10), and mutant homozygotes (lanes 2, 5, and 9) visible in this gel. The two ladders are visible in the middle (lane 7) and to the right (lane 14). **(B)** This gel shows the F3 generation (the offspring of mutant homozygotes from **Supplemental 1A**) along with wild-type controls in the middle (lanes 6 and 7) and ladders on the left and right ends. This was used to verify that the crossed strains had deletions in the *fzo-1* or *drp-1* gene.

For *fzo-1* (tm1133), the external primers will result in a band at either 2000 bp (wild-type) or 1600 bp (deletion). Internal tm1133 primers will have a band at either 1800 or 1400 bp. For the *fzo-1* mutant, the deletion is 421 bp and the insertion is 14 bp. For *drp-1* (tm1108) the primers will result in a band at either 2073 bp (wild-type) or 1665 bp (deletion). For the *drp-1* mutant, the deletion is 426 bp and the insertion is 18 bp.

Supplemental 2: Results of Other UVC Exposures

Serial UVC Exposure Information: I have data on an additional dose of serial UVC (2.5 J/m²), though this dosing and scoring was done at a different time (preliminary to all of the data presented in this thesis). The 2.5 J/m² dose still resulted in the larval arrest of the *fzo-1* strain. Moreover, when I recorded the neurodegeneration score for all the experiments in this thesis, I recorded whether the neuron was dorsal or ventral (if possible) in accordance to Claudia's instruction. In some cases it was impossible to determine if the neuron was dorsal or ventral (e.g., when there was a lot of neurodegeneration). This may be of use to look at in the future.

Additional Dosing of *fzo-1*: I dosed the *fzo-1* mutants at many different doses of UVC at the L1 stage to see if there was any dose at which they would not undergo complete larval arrest; I did not find that dose. The lowest doses I tried were 1.25 J/m² (about three seconds of exposure) and 2.5 J/m² (about five seconds of exposure). Every dose of UVC resulted in larval arrest of the *fzo-1* strain. I also dosed *fzo-1* deletion mutants at the L4 stage with one dose of 50 J/m² of UVC. They still underwent complete arrest, but it took them longer to reach this arrest than when dosed

as L1s (about 48 hours instead of 24 hours). However, even after 24 hours, they were still abnormal and displayed a marked reduction in movement.

Second Generation Experiment: I did another UVC experiment where I dosed worms with UVC during their development and then looked at neurodegeneration in the offspring. I dosed all three strains during their lifetime at the L1, L2, and L4 stages (i.e., immediately after plating synchronized L1s, 24 hours after plating, and 48 hours after plating). The different larval stages received equivalent doses of UVC (L1: dosed with 7.5 J/m^2 , L2: dosed with 10 J/m^2 , and L4: dosed with 50 J/m^2). The *fzo-1* underwent complete larval arrest. This experiment only consisted of one repetition with a very small sample size, so further reps will be necessary to make suitable conclusions and to determine statistical significance. The parents exhibited more neurodegeneration than their offspring; the UVC-exposed parents had scores of either 0 or 2 while the offspring had scores of either 0 or 0.5. The parent controls and offspring both had scores of 0 or 0.5. Given the amount of neurodegeneration I saw in my controls, human error is a possibility in this rep. It would also be necessary to repeat this experiment to take more care that the parents and offspring are not accidentally mixed up. However, given the very low levels of neurodegeneration in the offspring, this experiment may not culminate in interesting results.

Supplemental 3: 6-OHDA Exposure Protocol

About 150 worms at the L4 stage were exposed to each treatment. Counting of worms involved washing worms off plates with K⁺ medium into new 15 mL conicals. The caps were left off or loosened most of the time to ensure the worms were getting enough oxygen. Worms were

suspended into about 10 mL of K⁺ medium. Worms were resuspended and using a triton-coated pipette tip, three drops of 25 μ L were plated on to a slide. Triton was used on each tip to prevent worms from sticking on the tip. The number of worms in the 75 μ L of K⁺ were counted and a number of worms per μ L was calculated to determine the volume to add to each dosing tube to have 150 worms for each treatment.

A stock solution of 100 mM 6-OHDA (in ascorbic acid) was made for the dosing solutions. The ascorbic acid was made at a concentration of 20% of the concentration of the stock solution (so, 20 mM). Ascorbic acid was dissolved in K⁺. To reduce the likelihood of 6-OHDA oxidizing (and thus not working), precautions were taken to reduce the 6-OHDA's contact to light. The 6-OHDA solution was made in a 20 mL scintillation vial covered in aluminum foil, and during exposure, the tubes of worms and dosing solution were placed on a shaker in a 20 °C incubator in the dark.

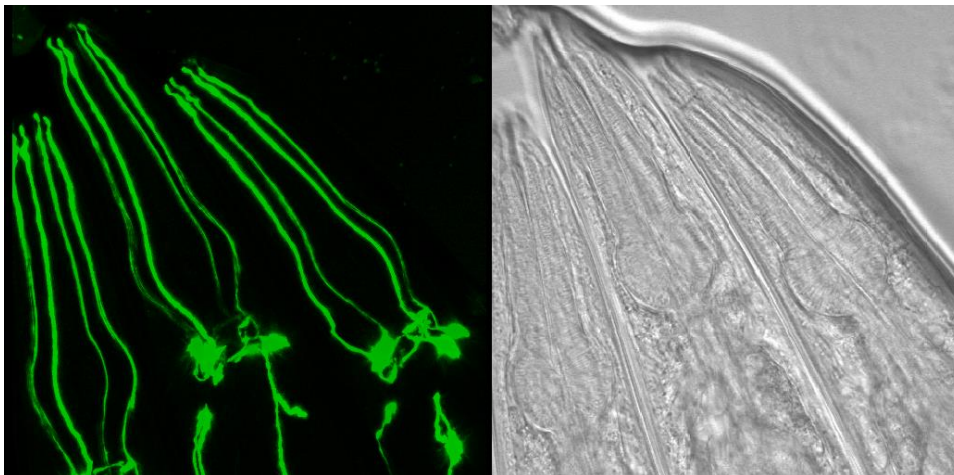
The total volume in each 1.5 mL dosing tube was 500 μ L (other protocols will dose in 1 mL, but I halved the number of worms and dosing solution so I would not use as much 6-OHDA). The worms in K⁺ accounted for 250 μ L (after counting and adding worms, K⁺ was added up to 250 μ L). The other 250 μ L was either 6-OHDA or ascorbic acid.

After 1 hour on a shaker in a 20 °C incubator, the tubes were spun down at 2200 rcf for 2 minutes and 450 μ L of the supernatant was removed and disposed into toxic waste. The worms were then washed with 900 μ L of K medium, before being spun down again. Washing occurred four times to completely remove the 6-OHDA. The worms were then plated on to K agar plates

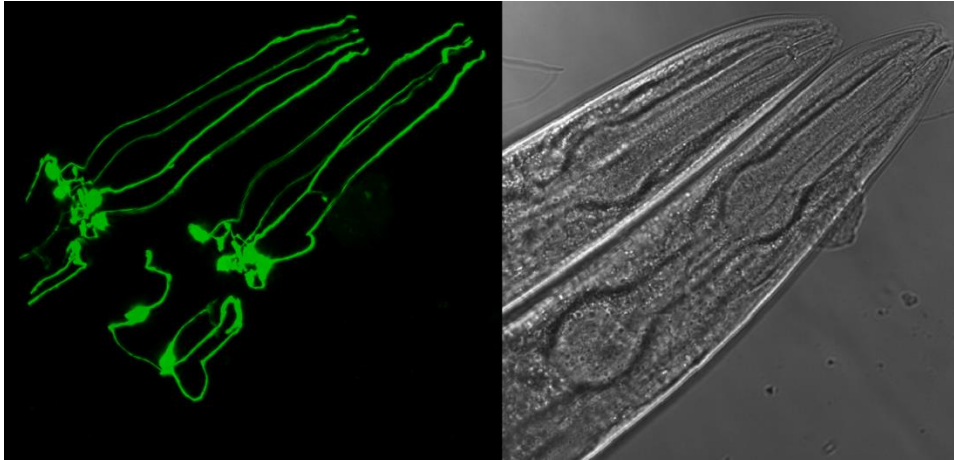
with food. Note that if the agar plates turned pink, then the 6-OHDA had not been completely removed, and the worms would have needed to be rewashed with K medium before plating on to food again.

Supplemental 4: Representative Confocal Images of Neurodegeneration

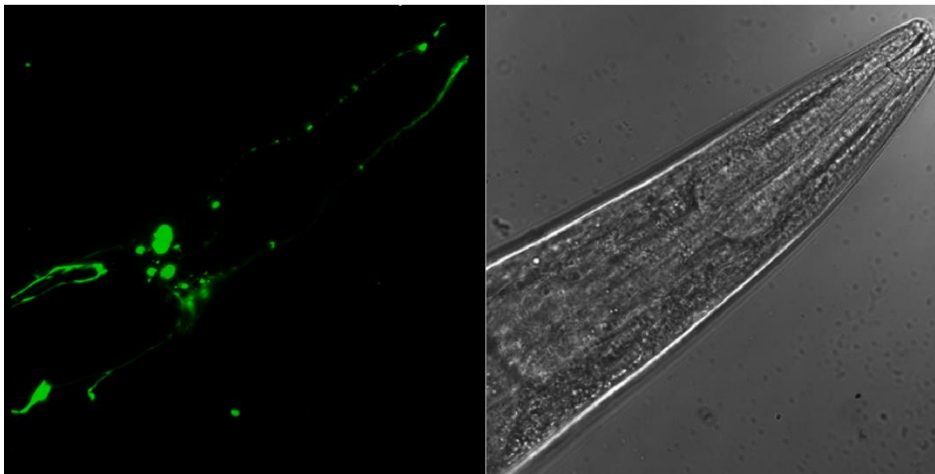
The following are representative confocal images of the worms I scored, to orient readers to the level of neurodegeneration I saw. The images depict the head region of adult *C. elegans*, with the fluorescent image on the left and the corresponding brightfield image on the right. Each worm will have four dendrites visible in the fluorescent image, unless there has been complete neurodegeneration. The images are ordered by the level of 6-OHDA exposure (unexposed controls, 50 mM, and 100 mM). There are no confocal images from worms exposed to UVC, and only BY250 and *drp-1* strains were imaged (for convenience, the *fzo-1* and UVC exposure were left out).



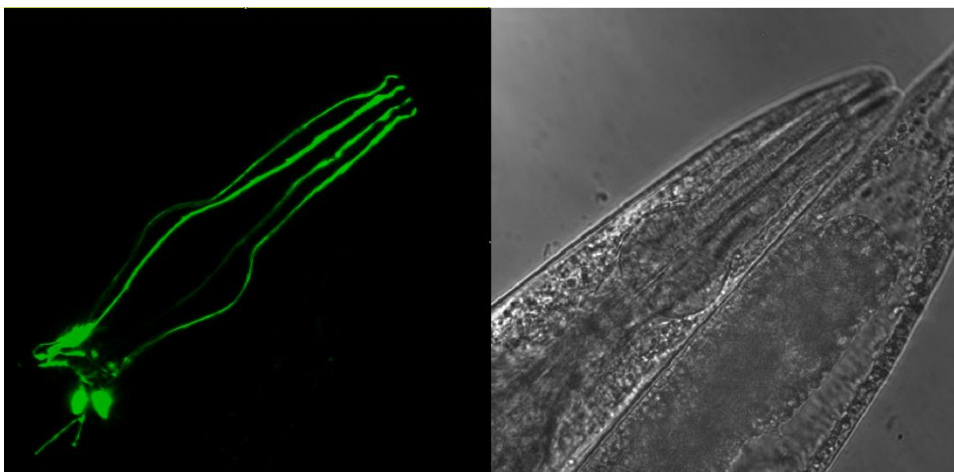
A) BY250 unexposed control. Three adult worms.



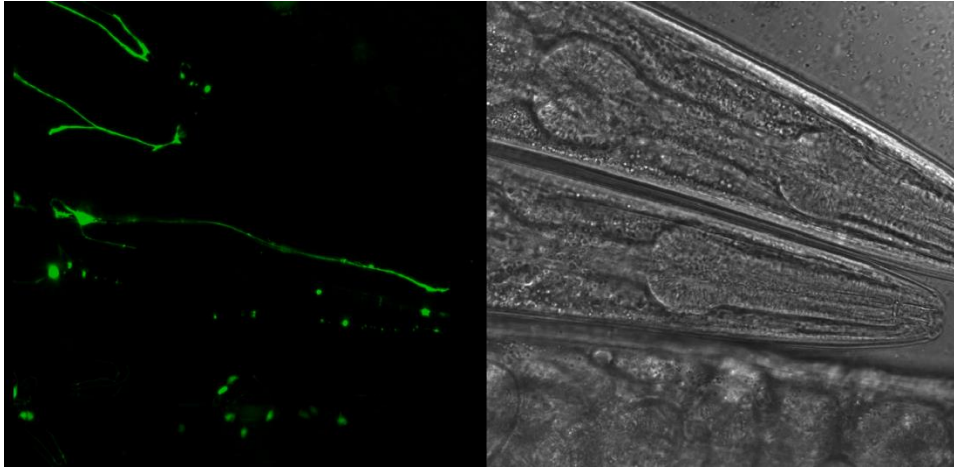
B) *drp-1* unexposed control. Two worms, and there is an outgrowth of the dendrite visible on the right worm.



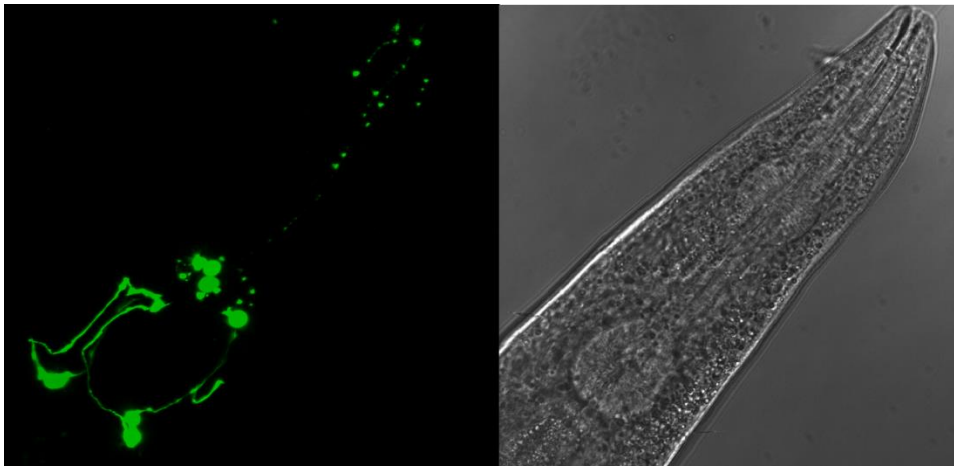
C) BY250 50 mM 6-OHDA.



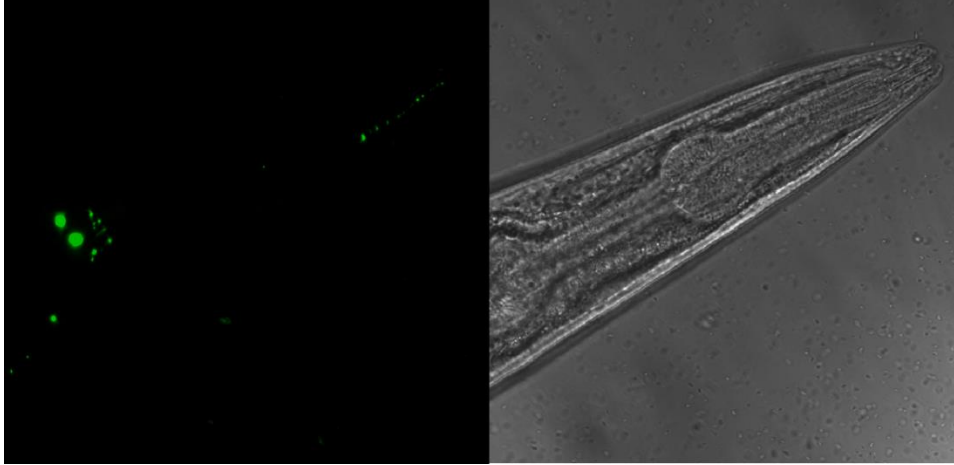
D) BY250 50 mM 6-OHDA. Note that the second worm visible in the lower right does not show a GFP signal because its head region is out of frame (and its dopaminergic neurons may have actually completely degenerated).



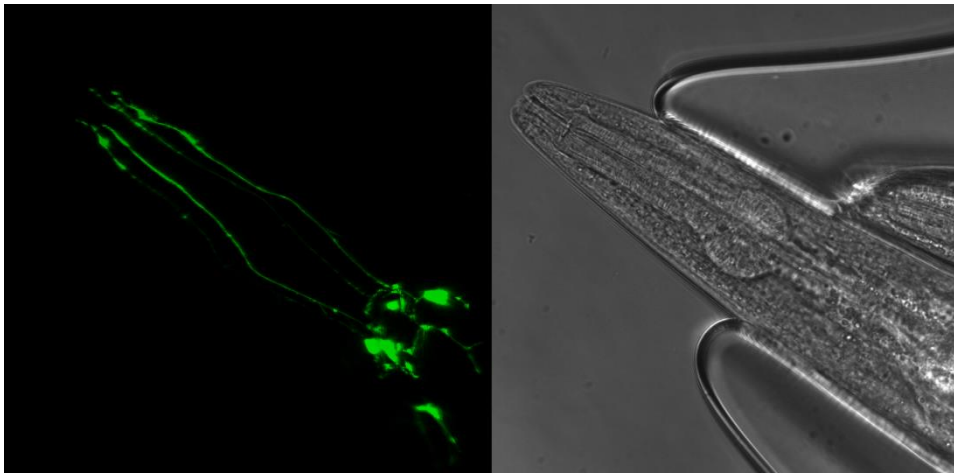
E) BY250 100 mM 6-OHDA. Three worms, with the dendrites visible in the top two. The topmost worm shows complete neurodegeneration. The third worm on the bottom of the frame is a gravid adult and there are several eggs visible (the eggs are late-stage and should have been laid, instead of developing so much inside the parent).



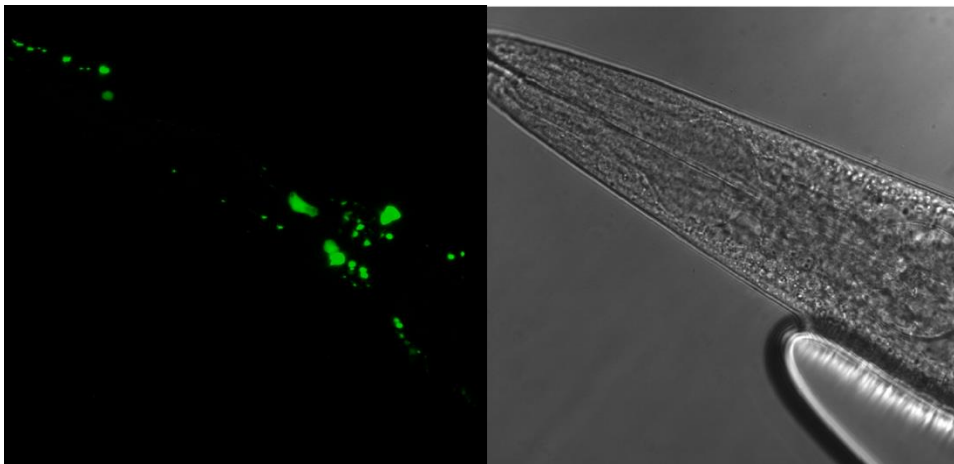
F) BY250 100 mM 6-OHDA. Blebbing is notable on all four dendrites, especially towards the nose.



G) BY250 100 mM 6-OHDA. This worm would be scored as a 2 because only a few blebs remain of the dendrite, and only two small, rounded cell bodies are visible instead of the normal four.



H) *drp-1* 100 mM 6-OHDA.



I) *drp-1* 100 mM 6-OHDA. This worm is actually dying.

Supplemental 5: Statistical Analysis

The effect of dose (strains by dose) was done through the Wilcoxon/Kruskal-Wallis Test. The effect of strain (doses by strain) was done through Fisher's Exact Test. The n value represents the sample size per treatment. Red font indicates statistical significance (p-value < 0.05).

6-OHDA 48 hours after dosing			6-OHDA 6 days after dosing		
Strains by Dose	p-value	n	Strains by Dose	p-value	n
BY250	<.0001*	180	BY250	<.0001*	180
drp-1	<.0001*	180	drp-1	<.0001*	180
fzo-1	<.0001*	180	fzo-1	<.0001*	180
Doses by Strain	p-value	n	Doses by Strain	p-value	n
Controls	<.0001*	180	Controls	.0087*	180
50 mM	<.0001*	180	50 mM	<.0001*	180
100 mM	<.0001*	180	100 mM	<.0001*	180

UVC 48 hours after dosing			UVC 96 hours after dosing			UVC 9 days after dosing		
Strains by Dose	p-value	n	Strains by Dose	p-value	n	Strains by Dose	p-value	n
BY250	<.0001*	180	BY250	<.0001*	179-240	BY250	<.0001*	168-180
drp-1	<.0001*	180	drp-1	.0012*	180-240	drp-1	.0047*	172-180
fzo-1	---	---	fzo-1	---	---	fzo-1	---	---
Doses by Strain	p-value	n	Doses by Strain	p-value	n	Doses by Strain	p-value	n
Controls	0.6938	180	Controls	.0068*	240	Controls	.0114*	180
7.5 J/m ²	0.2973	180	7.5 J/m ²	.0071*	179-180	7.5 J/m ²	.8769	176-180
10 J/m ²	<.0001*	180	10 J/m ²	.3515	180	10 J/m ²	.0222*	168-172